JCTC Journal of Chemical Theory and Computation

Article

pubs.acs.org/JCTC

Efficient Combination of Environment Change and Alchemical Perturbation within the Enveloping Distribution Sampling (EDS) Scheme: Twin-System EDS and Application to the Determination of Octanol–Water Partition Coefficients

Niels Hansen, Philippe H. Hünenberger, and Wilfred F. van Gunsteren*

Laboratory of Physical Chemistry, Swiss Federal Institute of Technology, ETH, CH-8093 Zürich, Switzerland

Supporting Information

ABSTRACT: The methodology of Enveloping Distribution Sampling (EDS) is extended to probe a single-simulation alternative to the thermodynamic cycle that is standardly used for measuring the effect of a modification of a chemical compound, e.g. from a given species to a chemical derivative for a ligand or solute molecule, on the free-enthalpy change associated with a change in environment, e.g. from the unbound state to the bound state for a protein–ligand system or from one solvent to another one for a solute molecule. This alternative approach relies on the coupled simulation of two systems (computational boxes) 1 and 2, and the method is therefore referred to as twin-system EDS. Systems 1 and 2 account for the two choices of environment. The end states of the alchemical perturbation for the twin-system associate the two alternative forms X and Y of the molecule to systems 1 and 2 or 2 and 1, respectively. In this way, the processes of transforming one molecule into the other are carried out simultaneously in opposite directions in the two environments, leading to a change in free enthalpy that is smaller than for the two individual processes and to an energy-difference distribution that is more symmetric. As an illustration, the method is applied to the calculation of octanol–water partition coefficients for C_4 to C_8 alkanes, 1-hexanol and 1,2-dimethoxyethane. It is shown in particular that the consideration of the residual hydration of octanol leads to calculated partition coefficients that are in better agreement with reported experimental numbers.

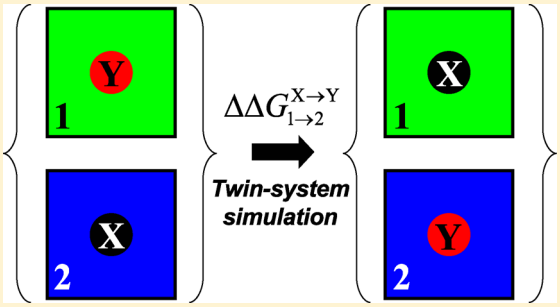

1. INTRODUCTION

The thermodynamic determinant of physicochemical processes such as protein–ligand binding or solute partitioning between different solvents is the corresponding change in free energy or rather free enthalpy[1] or Gibbs energy.[2] In the context of atomistic simulations, e.g., molecular dynamics (MD), a wide variety of methods to estimate free-enthalpy differences is nowadays available,[3−7] out of which the appropriate method has to be selected for the question at hand. A frequently occurring problem in (bio)chemistry is the estimation of the effect of a modification of a chemical compound, e.g., from a given species X to a modified species Y, on the change in free enthalpy associated with a change in environment, e.g., from the unbound state to the bound state for a protein–ligand system or from one solvent to another one for a solute molecule.

The usual way to address this problem computationally is displayed in the upper part of Figure 1. It involves the separate estimation of two free-enthalpy differences for the perturbation from X to Y in environments 1 and 2, respectively, using an appropriate free-enthalpy calculation method. If the method relies on a Hamiltonian coupling scheme defining a λ-parametrized path connecting X and Y, as is the case for thermodynamic integration (TI)[8] or staged free-energy perturbation (FEP),[9] the free enthalpy along this pathway is a function of λ, as illustrated by the green and blue curves in the upper right graph of Figure 1. The desired quantity $\Delta\Delta G_{1\to2}^{X\to Y} = \Delta G_{1\to2}^{Y} - \Delta G_{1\to2}^{X}$ is then obtained by closure of a thermodynamic cycle, in the form of the calculated difference $\Delta G_{2}^{X\to Y} - \Delta G_{1}^{X\to Y}$. In many cases, e.g., when creating or annihilating partial charges, this difference involves two numbers of comparable and large magnitudes, while the value of $\Delta\Delta G_{1\to2}^{X\to Y}$ itself is of significantly smaller magnitude. This is analogous to the situation where the weight of the captain is estimated by weighting the boat, with or without the captain on board. As a result, unnecessarily long simulation times may be required to reach sufficiently small uncertainties in the two individual free-enthalpy determinations.

In this article, an alternative method is proposed that involves the simultaneous simulation of two systems (computational boxes) corresponding to the two environments 1 and 2. The X to Y mutation in system 2 is carried out simultaneously with the Y to X mutation in system 1. The overall perturbation leads directly to $\Delta\Delta G_{1\to2}^{X\to Y}$, with large components of $\Delta G_{1}^{X\to Y}$ and $\Delta G_{2}^{X\to Y}$ canceling out, the cancellation being most effective

Received: October 27, 2012
Published: January 22, 2013

   dx.doi.org/10.1021/ct300933y | J. Chem. Theory Comput. 2013, 9, 1334–1346

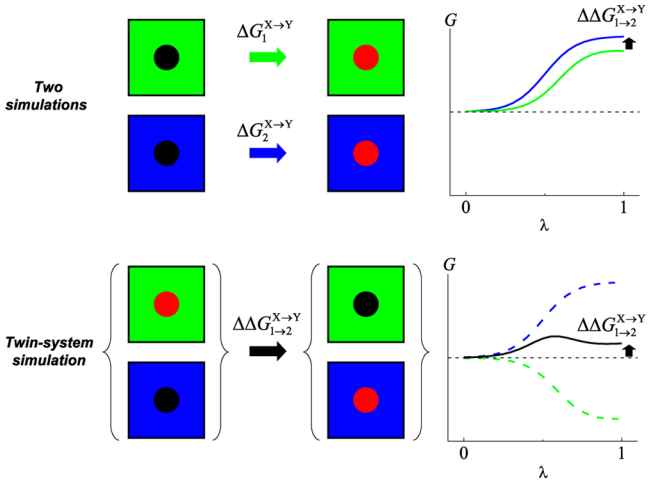

Figure 1. Illustration of two computational approaches to calculate a relative free enthalpy of transfer $\Delta\Delta G_{1\to 2}^{X\to Y} = \Delta G_{1\to 2}^{Y} - \Delta G_{1\to 2}^{X}$, where X→Y represents an alchemical perturbation from species X to species Y and 1→2 represents a transfer from environment 1 to environment 2. In both cases, the difference is calculated by closure of a thermodynamic cycle, in the form $\Delta\Delta G_{1\to 2}^{X\to Y} = \Delta G_2^{X\to Y} - \Delta G_1^{X\to Y}$. The usual computational solution, illustrated in the upper part, involves two separate calculations of $\Delta G_1^{X\to Y}$ and $\Delta G_2^{X\to Y}$ using an appropriate free-enthalpy calculation method, typically resulting in two numbers of large and comparable magnitudes that are to be subtracted. The twin-system approach proposed in the present work, illustrated in the lower part, relies on the simultaneous simulation of two systems (computational boxes) corresponding to the two environments and couples the X→Y mutation in system 2 to the Y→X mutation in system 1. The overall perturbation leads directly to $\Delta\Delta G_{1\to 2}^{X\to Y}$, with a large component of $\Delta G_1^{X\to Y}$ and $\Delta G_2^{X\to Y}$ canceling out.

when the two environments are similar. This approach, referred to here as the twin-system approach, is illustrated in the lower part of Figure 1. The twin-system free enthalpy as a function of λ, represented by the black curve in the lower right graph of Figure 1, is much flatter than the curves representing the individual processes and, therefore, in principle is easier to calculate accurately. The working principle of the twin-system approach is analogous to that of a cable car: the work required is reduced by coupling a car that is going uphill (X to Y) with a car that is going downhill (Y to X), the net work being formally determined by the different weights of the passengers in the two cars, analogous to the environment difference in the present case. In the special situation where the two environments 1 and 2 are the same, one expects $\Delta\Delta G_{1\to 2}^{X\to Y} = 0$. This does not imply, however, that the corresponding free-enthalpy profile as a function of λ is entirely flat, which will only be the case if the corresponding single-mutation profile is linear.

The twin-system approach is not bound to a particular method to compute free-enthalpy differences. In the present work, it is realized in the framework of the Enveloping Distribution Sampling (EDS) methodology.[10−16] Note that this specific method does not involve any coupling parameter λ. The approach is illustrated here by calculating partition coefficients for a number of small solute molecules in the octanol−water system.

Partition coefficients of organic solutes in the octanol−water system are widely employed in drug design,[17,18] environmental risk assessment,[19] and medicinal chemistry[20] to characterize the lipophilicity of a given compound. Due to their importance, significant effort has been devoted to the development of simple methods for their prediction, or that of solvation free enthalpies, based on additive group-contribution schemes,[21−28] on approximate linear correlations to solute molecular properties as in quantitative structure−property models[29−35] (QSPR), or to experimental properties as in property−property relationship models[36] (PPR), or on continuum-solvation models.[37−43]

Molecular simulations based on classical force fields are also commonly used to calculate parameters related to solvation thermodynamics, such as partition or activity coefficients.[44−46] Although this approach cannot compete with the simpler methods listed above in terms of computational cost, it becomes the only viable alternative for complex liquid−liquid equilibrium problems where simple methods are reaching their limits,[47,48] either due to a lack of available parameters[49] or because information on the conformational distribution of the solute becomes important.[50−53]

The partition coefficient P_{12}^{X} of a species X between two phases 1 and 2 is defined by the ratio c_1/c_2 of the corresponding equilibrium concentrations and is related to the associated free enthalpy of transfer $\Delta G_{1\to 2}^{X}$ as[54]

$$\Delta G_{1\to 2}^{X} = RT \ln P_{12}^{X} \tag{1}$$

where R is the ideal-gas constant and T the absolute temperature. Both quantities are in principle functions of pressure, temperature and concentration (c_1 or c_2), and typically reported for atmospheric pressure, room temperature, and in the limit of infinite dilution.[55] It is important to stress that P_{12}^{X} refers to a ratio of molar concentrations (mole X per unit volume) irrespective of the nature of the two phases. Most commonly, these phases will consist of two essentially immiscible solvents. However, even limited mutual solubility of the solvents induces an ambiguity concerning the nature of the quantities involved, i.e., whether they refer to pure 1 and pure 2 solvents or to 2-saturated 1 and 1-saturated 2 phases. For the partitioning between 1-octanol and water, the partition coefficient of a given solute X, usually expressed in the form of $\log P_{OW}^{X}$, where log is a decadic logarithm, is given by

$$\log P_{OW}^{X} = \frac{\Delta G_{W}^{X} - \Delta G_{O}^{X}}{RT \ln 10} \tag{2}$$

where ΔG_{W}^{X} denotes the hydration free enthalpy of the solute, i.e., its solvation free enthalpy in water, and ΔG_{O}^{X} its solvation free enthalpy in 1-octanol.

In the context of classical molecular simulations, partition coefficients can be calculated by Monte Carlo or MD simulations. A single-simulation approach of the former type is the Gibbs ensemble Monte Carlo (GEMC) method,[56] usually in its constant pressure formulation,[57] utilizing two (or more) computational boxes which are in thermodynamic contact but do not have an explicit interface. By performing particle-exchange and switch moves, usually carried out by the configurational-bias Monte Carlo (CBMC) technique,[58−60] the chemical potentials of each species in the two phases are equalized.[61,62] The composition of the two solvent phases does not need to be specified in advance because the distribution of solvent molecules is also sampled *via* particle-exchange moves. The free enthalpy of transfer is directly determined from the ratio of solute number densities in the two phases.[63,64] Alternatively, if the configurational ensemble is generated by MD, partition coefficients are often calculated from solvation free enthalpies in the two different solvents, determined e.g. by

TI at fixed compositions of the two phases.[65−67] While this methodology is well established, it is computationally expensive and may require a considerable amount of human time to optimize the TI protocol, including the choice of the λ-dependence of the Hamiltonian,[68] the λ-point distribution,[69] as well as equilibration and sampling times at the different points, so as to reach converged free-enthalpy estimates.[65−67,70] Given a set of solutes of similar sizes, an alternative route is to calculate relative solvation free enthalpies *via* the alchemical transformation of one solute into another in both solvents by means of e.g. FEP.[71,72] Solvation free enthalpies, and thus partition coefficients, can then be derived provided that the solvation free enthalpies of a single reference compound in the two solvents are known, e.g., as obtained by the above TI method. The latter approach is computationally more efficient provided that the FEP calculations converge on a reasonable time scale. In practice, this limits the degree by which the solutes of interest may deviate from the reference compound.[73] If the alchemical perturbation induces a considerable reorganization of the solvent molecules, the FEP method is subject to convergence problems,[37] necessitating the use of staging approaches.[74] It is therefore of interest to study alternative free-enthalpy methods[61,75−78] that are applicable to larger perturbations but have the potential to be more efficient than additional TI calculations for the estimation of relative partition coefficient.

The EDS method was shown previously to be a powerful alternative to TI in a variety of applications, ranging from the study of protein−ligand binding[14] to folding free-enthalpy predictions.[15] Its strengths are that (*i*) no pathway has to be defined between two end states, (*ii*) no intermediate states are required, and (*iii*) several measures to assess the quality of sampling can be employed.[16] Limitations of the method are imposed by the magnitude of the perturbation, which affects the computational overhead associated with the precalculation of EDS parameters guaranteeing a sufficient sampling of both end states during the EDS reference-state simulation.

In the present work, the twin-system EDS approach is used to calculate octanol−water partition coefficients of short (C_4−C_8) alkanes, 1-hexanol, and 1,2-dimethoxyethane. Results obtained using different versions of the GROMOS force field[79−82] are compared, as well as partition coefficients calculated considering dry and wet octanol phases, and related to other simulation studies from the literature.

2. THEORY

2.1. Calculation of Partition Coefficients. As illustrated in Figure 2, the octanol−water partition coefficient of a solute X (eq 2) can be expressed as

$$\begin{aligned}\log P_{\mathrm{OW}}^{\mathrm{X}} &= \frac{\Delta G_{\mathrm{W}}^{\mathrm{X}} - \Delta G_{\mathrm{O}}^{\mathrm{X}}}{RT \ln 10} \\ &= \frac{\Delta G_{\mathrm{W}}^{\mathrm{M}'\to\mathrm{M}} + \Delta G_{\mathrm{W}}^{\mathrm{M}\to\mathrm{X}} - (\Delta G_{\mathrm{O}}^{\mathrm{M}'\to\mathrm{M}} + \Delta G_{\mathrm{O}}^{\mathrm{M}\to\mathrm{X}})}{RT \ln 10} \\ &= \log P_{\mathrm{OW}}^{\mathrm{M}} + \frac{\Delta G_{\mathrm{W}}^{\mathrm{M}\to\mathrm{X}} - \Delta G_{\mathrm{O}}^{\mathrm{M}\to\mathrm{X}}}{RT \ln 10} \\ &= \log P_{\mathrm{OW}}^{\mathrm{M}} + \frac{\Delta\Delta G_{\mathrm{O}\to\mathrm{W}}^{\mathrm{M}\to\mathrm{X}}}{RT \ln 10}\end{aligned} \tag{3}$$

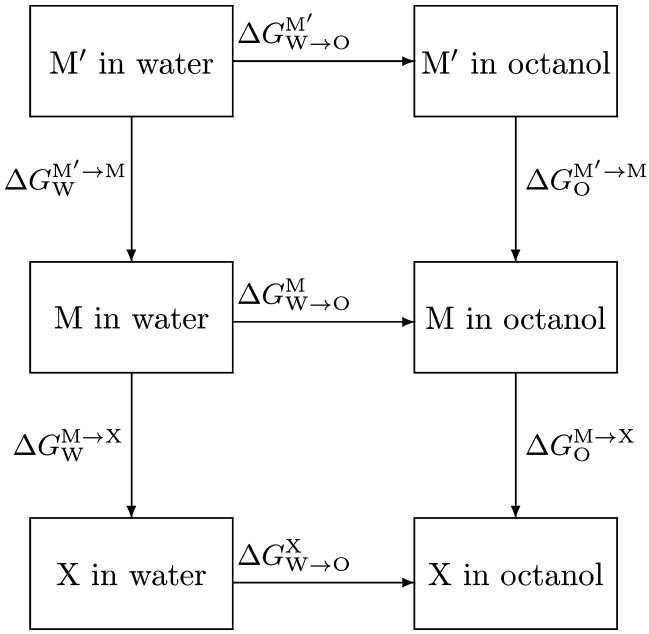

Figure 2. Thermodynamic cycles for the calculation of the octanol−water partition coefficient of a reference solute M and a target solute X, where M′ denotes the reference solute possessing full intramolecular interactions but exempt of interactions with the solvent. The vertical branches labeled $\Delta G_{\mathrm{W}}^{\mathrm{M}'\to\mathrm{M}}$ and $\Delta G_{\mathrm{O}}^{\mathrm{M}'\to\mathrm{M}}$ represent the solvation free enthalpy of the reference solute in water and octanol, respectively. The vertical branches labeled $\Delta G_{\mathrm{W}}^{\mathrm{M}\to\mathrm{X}}$ and $\Delta G_{\mathrm{O}}^{\mathrm{M}\to\mathrm{X}}$ represent the changes in free enthalpy associated with the alchemical perturbation of the reference solute M to the target solute X in water and octanol, respectively. The horizontal branches represent the transfer free enthalpies for the different species from water to octanol. Note that $\Delta G_{\mathrm{W}\to\mathrm{O}}^{\mathrm{M}'} = 0$.

where M represents a solute used as reference compound and M′ represents the corresponding molecule possessing full intramolecular interactions but exempt of interactions with the solvent. The superscript/subscript notations indicate the solvation free enthalpy of X in phase 1 (ΔG_1^{X}), the mutation free enthalpy of X to Y in phase 1 ($\Delta G_1^{\mathrm{X}\to\mathrm{Y}}$), the transfer free enthalpy of X from phase 1 to phase 2 ($\Delta G_{1\to2}^{\mathrm{X}}$), and the free enthalpy difference $\Delta G_{1\to2}^{\mathrm{Y}} - \Delta G_{1\to2}^{\mathrm{X}} = \Delta G_2^{\mathrm{X}\to\mathrm{Y}} - \Delta G_1^{\mathrm{X}\to\mathrm{Y}}$ ($\Delta\Delta G_{1\to2}^{\mathrm{X}\to\mathrm{Y}}$). In particular, $\Delta G_{\mathrm{W}}^{\mathrm{X}}$ denotes the hydration free enthalpy of the solute X and $\Delta G_{\mathrm{O}}^{\mathrm{X}}$ its solvation free enthalpy in octanol. In eq 3, these free enthalpies are decomposed into contributions from activating the solute−solvent interactions of the noninteracting reference solute M′ to the fully interacting reference solute M, $\Delta G_{\mathrm{S}}^{\mathrm{M}'\to\mathrm{M}}$ (S = W,O), and the free enthalpy changes associated with an alchemical perturbation of M to X performed in water and octanol, $\Delta G_{\mathrm{S}}^{\mathrm{M}\to\mathrm{X}}$ (S = W,O), using the fact that $\Delta G_{\mathrm{W}\to\mathrm{O}}^{\mathrm{M}'} = 0$. The last term on the right-hand side of eq 3 is a relative partition coefficient that can be calculated directly using the twin-system approach as illustrated in Figure 3, which involves the simultaneous simulation of two distinct systems, i.e., two distinct computational boxes. In this coupled perturbation, the initial state A combines the system containing the reference solute solvated in octanol (system 2) with the system containing the target solute solvated in water (system 1), while the final state B combines the system containing the target solute solvated in octanol (system 2) with the system containing the reference solute solvated in water (system 1).

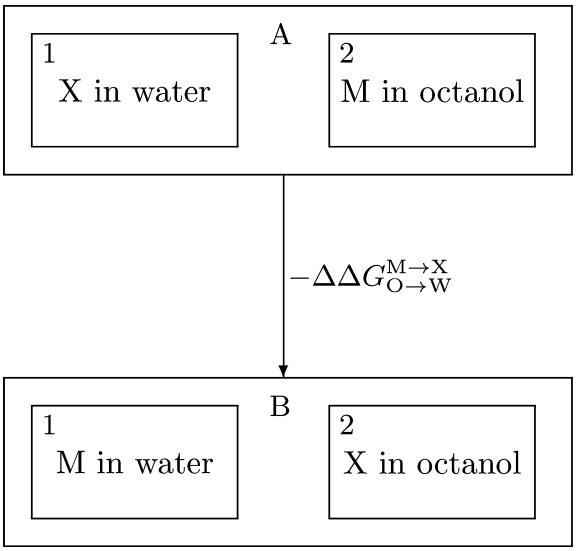

Figure 3. Illustration of the twin-system approach for the calculation of the relative octanol–water partition coefficient associated with the alchemical perturbation from solute M to solute X. The indices 1 and 2 denote the two separate systems (computational boxes) involving the different solvents while the two different states of the twin-system are labeled A and B.

The overall process involves the two subprocesses of changing solute M to solute X in the two solvents, carried out simultaneously in opposite directions, yielding directly $\Delta G_O^{M\to X} - \Delta G_W^{M\to X} = -\Delta\Delta G_{O\to W}^{M\to X}$. This twin-system approach can conveniently be realized using the EDS methodology as outlined below.

2.2. Enveloping Distribution Sampling (EDS). The EDS scheme is a special form of the umbrella sampling approach[83] that focuses the sampling on the relevant phase space of a system presenting N_H different states n using a reference Hamiltonian H_R defined as[11,84−86]

$$H_R(\mathbf{r}, \mathbf{p}) = -\frac{1}{\beta s} \ln \sum_{n=1}^{N_H} e^{-\beta s(H_n(\mathbf{r},\mathbf{p}) - E_n^R)} \tag{4}$$

where $\mathbf{r}$ and $\mathbf{p}$ denote the $3N$-dimensional vector of spatial coordinates and the $3N$-dimensional vector of conjugate momenta, respectively, N being the number of atoms in the system, and $\beta = 1/k_B T$, k_B being the Boltzmann constant and T the absolute temperature. The smoothness parameter s ($0 < s \leq 1$) controls the barriers determining the rate of transitions between the different states n. The energy offsets E_n^R of the different states serve to bring their energies to the same level for homogeneous sampling. These parameters have to be determined iteratively prior to the EDS production simulation.[12,14,16] The free-enthalpy difference between a pair of states (n, m) is calculated based on this production simulation using

$$G_n - G_m = -\frac{1}{\beta} \ln \frac{\langle e^{-\beta(H_n(\mathbf{r},\mathbf{p}) - H_R(\mathbf{r},\mathbf{p}))} \rangle_R}{\langle e^{-\beta(H_m(\mathbf{r},\mathbf{p}) - H_R(\mathbf{r},\mathbf{p}))} \rangle_R} \tag{5}$$

where $\langle ... \rangle_R$ denotes ensemble averaging over a simulation generated using the reference-state Hamiltonian H_R (eq 4).

Note that, although the word "reference" is used both for the reference compound M used in the evaluation of relative partition coefficients and the EDS reference state R, the two concepts are entirely distinct and should not be confused.

2.3. Twin-System EDS. In the twin-system EDS approach, considering the situation depicted in Figure 3, both end states A and B of the twin-system are composed of two separate systems (1 and 2) in opposite alchemical states. The Hamiltonian of state n (n = A,B) is then obtained as the sum of the Hamiltonians of the two systems

$$H_n = H_{n1} + H_{n2} \tag{6}$$

Note that these Hamiltonians are functions of vectors $\mathbf{r}$ and $\mathbf{p}$ that account for the coordinates and momenta of the particles in the two systems. As a result, the potential energy term of the EDS reference-state Hamiltonian (eq 4) reads

$$V_R(\mathbf{r}; s, \Delta E_{BA}^R) = -\frac{1}{\beta s} \ln[e^{-\beta s(V_{A1}(\mathbf{r}) + V_{A2}(\mathbf{r}) - E_A^R)} + e^{-\beta s(V_{B1}(\mathbf{r}) + V_{B2}(\mathbf{r}) - E_B^R)}] \tag{7}$$

where $\Delta E_{BA}^R = E_B^R - E_A^R$ denotes the relative energy offset. Accordingly, the force on an atom i at coordinate $\mathbf{r}_i$ is given by

$$\begin{aligned}\mathbf{f}_i(t) &= \left(-\frac{\partial V_R(\mathbf{r})}{\partial \mathbf{r}_i}\right) \\ &= [1 + e^{-\beta s(V_{B1}(\mathbf{r}) + V_{B2}(\mathbf{r}) - (V_{A1}(\mathbf{r}) + V_{A2}(\mathbf{r})) - \Delta E_{BA}^R)}]^{-1} \left(-\frac{\partial (V_{A1}(\mathbf{r}) + V_{A2}(\mathbf{r}))}{\partial \mathbf{r}_i}\right) \\ &\quad + [1 + e^{+\beta s(V_{B1}(\mathbf{r}) + V_{B2}(\mathbf{r}) - (V_{A1}(\mathbf{r}) + V_{A2}(\mathbf{r})) - \Delta E_{BA}^R)}]^{-1} \left(-\frac{\partial (V_{B1}(\mathbf{r}) + V_{B2}(\mathbf{r}))}{\partial \mathbf{r}_i}\right)\end{aligned} \tag{8}$$

Because the potential energy of system 1 does not depend on the configuration of system 2 and vice versa, one has

$$\frac{\partial V_{A2}}{\partial \mathbf{r}_i} = \frac{\partial V_{B2}}{\partial \mathbf{r}_i} = 0 \text{ for atoms } i \text{ in system 1}$$

$$\frac{\partial V_{A1}}{\partial \mathbf{r}_i} = \frac{\partial V_{B1}}{\partial \mathbf{r}_i} = 0 \text{ for atoms } i \text{ in system 2} \tag{9}$$

and eq 8 simplifies to

$$\begin{aligned}\mathbf{f}_{i1}(t) &= \left(-\frac{\partial V_R(\mathbf{r})}{\partial \mathbf{r}_i}\right) \\ &= [1 + e^{-\beta s(V_{B1}(\mathbf{r}) + V_{B2}(\mathbf{r}) - (V_{A1}(\mathbf{r}) + V_{A2}(\mathbf{r})) - \Delta E_{BA}^R)}]^{-1} \left(-\frac{\partial V_{A1}(\mathbf{r})}{\partial \mathbf{r}_i}\right) \\ &\quad + [1 + e^{+\beta s(V_{B1}(\mathbf{r}) + V_{B2}(\mathbf{r}) - (V_{A1}(\mathbf{r}) + V_{A2}(\mathbf{r})) - \Delta E_{BA}^R)}]^{-1} \left(-\frac{\partial V_{B1}(\mathbf{r})}{\partial \mathbf{r}_i}\right)\end{aligned} \tag{10}$$

for the force on an atom i in system 1 and to

$$\begin{aligned}\mathbf{f}_{i2}(t) &= \left(-\frac{\partial V_R(\mathbf{r})}{\partial \mathbf{r}_i}\right) \\ &= [1 + e^{-\beta s(V_{B1}(\mathbf{r}) + V_{B2}(\mathbf{r}) - (V_{A1}(\mathbf{r}) + V_{A2}(\mathbf{r})) - \Delta E_{BA}^R)}]^{-1} \left(-\frac{\partial V_{A2}(\mathbf{r})}{\partial \mathbf{r}_i}\right) \\ &\quad + [1 + e^{+\beta s(V_{B1}(\mathbf{r}) + V_{B2}(\mathbf{r}) - (V_{A1}(\mathbf{r}) + V_{A2}(\mathbf{r})) - \Delta E_{BA}^R)}]^{-1} \left(-\frac{\partial V_{B2}(\mathbf{r})}{\partial \mathbf{r}_i}\right)\end{aligned} \tag{11}$$

for the force on an atom i in system 2. Therefore, the coupling between the two systems only occurs *via* the prefactors and does not affect the evaluation of the derivative of the potential energy functions V_{n1} and V_{n2}.

2.4. Convergence Assessment. The time series of the potential energies of states A and B, $V_A(t)$ and $V_B(t)$, sampled in the reference-state ensemble R are obtained as the sum of the contributions from each system. In the reference-state ensemble R, the corresponding distribution of the energy difference ΔV_{BA} between the two end states can be calculated as[87,88]

$$\rho_R(\Delta V_{BA}) = \langle \delta[\Delta V_{BA} - (V_B(\mathbf{r}) - V_A(\mathbf{r}))] \rangle_R \quad (12)$$

where δ is the Dirac delta function (approximated in practice by a histogram-binning function). This distribution can be converted to predicted distributions, denoted by a tilde, corresponding to the end-state ensembles A or B *via* reweighting[89,90]

$$\tilde{\rho}_n(\Delta V_{BA}) = \frac{\langle \delta[\Delta V_{BA} - (V_B(\mathbf{r}) - V_A(\mathbf{r}))] e^{-\beta(V_n(\mathbf{r}) - V_R(\mathbf{r}))} \rangle_R}{\langle e^{-\beta(V_n(\mathbf{r}) - V_R(\mathbf{r}))} \rangle_R} \quad (13)$$

with n = A or B, respectively. The distributions given by eqs 12 and 13 are used to gain insight into the quality of the sampling obtained in the EDS simulation.[16]

In a similar manner, distributions of the potential energies V_A and V_B sampled in the reference-state ensemble R, $\rho_R(V_n)$, can be converted to predicted distributions corresponding to the end-state ensembles A or B, $\tilde{\rho}_n(V_n)$. These predicted distributions can be compared to actual distributions $\rho_n(V_n)$ based on independent simulations at the two end states and thus used for further assessment of the quality of the sampling obtained in the EDS simulation.[91]

3. COMPUTATIONAL DETAILS

3.1. Simulation Parameters. All MD simulations were carried out using a modified version of the GROMOS11 program package.[92−95] The solute molecules considered were butane, pentane, hexane, heptane, octane, 1-hexanol, and 1,2-dimethoxyethane. The GROMOS force-field parameter sets employed were 54A7,[79,80] 53A6$_{OXY}$,[81] and 53A6$_{OXY+D}$.[82] For the compounds considered here, there is no difference between the 54A7 version and the former major revision of the GROMOS force field, 53A6.[96] The 53A6$_{OXY}$ version differs from 54A7 for the alcohols and ethers, owing to a reparametrization of oxygen-containing chemical functions. The 53A6$_{OXY+D}$ version is equivalent to 53A6$_{OXY}$, the only difference involving improved torsional-energy parameters for the vicinal diether function, relevant here for 1,2-dimethoxyethane only. The covalent and nonbonded interaction parameters used in the present work are summarized in Figure S1 and Table S1, respectively, of the Supporting Information.

The simulations were performed under periodic boundary conditions based on cubic computational boxes containing one solute molecule solvated in 999 simple point charge[97] (SPC) water molecules, in 511 octanol molecules (dry octanol), or in a mixture consisting of 511 octanol and 100 water molecules (wet octanol). The latter situation is meant to account for the residual hydration of octanol in an experimental setup. The reason for using a water mole fraction of 0.16, below the experimental saturation concentration[20] of about 0.27, is that the simulated value of the saturation concentration depends on the quality of the force field and was reported to be lower than the experimental value for the TIP4P/TraPPE-UA (0.21),[62] TIP4P/OPLS (0.09)[61] and a modified 45A3 version of the GROMOS force field (0.16).[98] By using a water mole fraction of 0.16, the simulation of an oversaturated mixture is avoided, while the effect of water on the calculated partition coefficients is still observable. For 1,2-dimethoxyethane, simulations in a mixture of 511 octanol and 190 water molecules, resembling the experimental water mole fraction of 0.27 at saturation, were also carried out for comparison. However, the effect on the calculated partition coefficient compared to the corresponding simulation at a water mole fraction of 0.16 was found to be small.

The equations of motion were integrated using the leapfrog scheme[99] with a time step of 2 fs. Bond lengths and the bond angles of water molecules were constrained by application of the SHAKE procedure[100] with a relative geometric tolerance of 10^{-4}. The center of mass translation of the computational box was removed every 2 ps. All simulations were performed at constant pressure and temperature. The temperature was maintained at 298 K by weak coupling to an external bath[101] with a relaxation time of 0.1 ps. Solute and solvent were coupled to separate heat baths. The pressure was calculated using a group based virial and held constant at 1 atm using the weak coupling method with a relaxation time of 0.5 ps[101] and an isothermal compressibility κ_T of 7.513×10^{-4} (kJ mol^{-1} nm^{-3})$^{-1}$ for water,[102] 7.64×10^{-4} (kJ mol^{-1} nm^{-3})$^{-1}$ for dry octanol,[103] and 7.62×10^{-4} (kJ mol^{-1} nm^{-3})$^{-1}$ for wet octanol (composition-weighted average of the two former values).

The nonbonded van der Waals and electrostatic interactions were calculated using a twin-range cutoff scheme,[104] with short- and long-range cutoff distances set to 0.8 and 1.4 nm, respectively. The short-range interactions were calculated every time step using a group-based pairlist updated every fifth time step. The intermediate-range interactions were re-evaluated at each pairlist update and assumed constant in between. A reaction-field correction[105,106] was applied to account for the mean effect of electrostatic interactions beyond the long-range cutoff distance, using the experimental relative dielectric permittivities ε_{RF} of 78.5 for water,[102] 10.1 for dry octanol,[107] and 9.0 for wet octanol, appropriate for a water mole fraction of 0.16.[108−110] The reaction-field self-term and excluded-atom-term contributions to the energy, forces, and virial were included as described previously.[111]

3.2. Simulated Systems. End-state simulations, i.e., plain MD simulations of the seven compounds considered, solvated in water, dry octanol, or wet octanol, were conducted to determine the distributions of the solute−solute plus solute−solvent nonbonded energies. These distributions can be compared to those obtained from the EDS reference-state simulations *via* reweighting, which allows for an assessment of the quality of the sampling in the EDS reference-state simulations. The end-state simulations were carried out for 10 ns (30 ns for 1,2-dimethoxyethane) after 1 ns equilibration, and energies were written to file every 4 ps.

In the present work, the twin-system EDS approach is used to evaluate the relative effect caused by the perturbation of a reference compound M to a target compound X on the free-enthalpy change associated with a change of environment from O to W, $\Delta\Delta G_{O\rightarrow W}^{M\rightarrow X}$. To obtain partition coefficients *via* eq 3, the hydration free enthalpy of the reference compound M has to be known as well as its solvation free enthalpy in octanol, i.e., the change in free enthalpy for the process M′ → M (vertical

Table 1. Free Enthalpies of Hydration, ΔG_W, and Solvation Free Enthalpies in Dry and Wet Octanol, ΔG_{dO} and ΔG_{wO}, Respectively, from MD Simulations and Experimental Measurements[a]

	54A7			$53A6_{OXY(+D)}$		experiment		
solute	ΔG_W	ΔG_{dO}	ΔG_{wO}	ΔG_W	ΔG_{wO}	ΔG_W	ΔG_{dO}	ΔG_{wO}
hexane	10.5 ± 0.8	−14.6 ± 1.0	−13.2 ± 1.2	10.5 ± 0.8	−13.2 ± 1.0	10.40[b]	−13.89[c]	−11.86[d]
hexanol	−17.3 ± 0.9	−33.1 ± 1.6	−32.5 ± 1.7	−16.7 ± 1.0	−31.0 ± 1.6	−18.26[b]	−28.60[e]	−30.11[f]
$hexane_{+D}$				8.6 ± 0.8	−15.8 ± 1.0[g]			

[a]Free enthalpies (in kJ mol^{-1}) are reported for the solute molecules hexane, hexanol, and hexane with modified torsional-energy parameters ($hexane_{+D}$) based on a unit molarity (1 mol dm^{-3}) standard state for the gas and solution phases.[135] The simulated values are obtained using TI and rely on the 54A7[79,80] or $53A6_{OXY}$[81]/$53A6_{OXY+D}$[82] versions of the GROMOS force field. [b]Ref 23. [c]Ref 124. [d]Calculated from the value reported for dry octanol and the transfer free enthalpy $\Delta G_{dO\rightarrow wO}$ = +2.03 kJ mol^{-1} reported in ref 123. [e]Calculated from the value reported for wet octanol and an estimated transfer free enthalpy $\Delta G_{dO\rightarrow wO}$ = −1.50 kJ mol^{-1} based on reported[125] values of −1.76 and −1.36 kJ mol^{-1} for butanol and octanol, respectively. [f]Ref 126. [g]For this compound, an additional TI calculation considering an octanol−water mixture with a water mole fraction of 0.27 (experimental saturation concentration), instead of 0.16, resulted in the same (within two digits) ΔG_{wO} value.

branches in the upper part of Figure 2). In this work, hexane was chosen as a reference compound as it represents best the average number of atoms in the seven solute molecules considered. The calculation of the hydration free enthalpy of hexane and of its solvation free enthalpy in octanol relied on thermodynamic integration[8] over the average of the derivative of the Hamiltonian with respect to a scaling parameter λ applied to the solute−solvent interactions, from no interaction at $\lambda = 0$ to full interaction at $\lambda = 1$. The λ-coupling was chosen to be quadratic and involves a soft-core scaling[112] with $\alpha_{LJ} = 0.5$ and $\alpha_{CRF} = 0.5$ nm^2 for the Lennard-Jones and electrostatic interactions, respectively. The solute−solvent interactions were gradually activated using 21 equispaced λ-points with a sampling period of 1.8 ns after 0.2 ns equilibration. The Hamiltonian derivatives were written to file every 0.5 ps. The integration was performed using the trapezoidal rule. Errors in the individual ensemble averages for the Hamiltonian derivative were calculated by block-averaging[113] and propagated into an error estimate for the free enthalpy according to the trapezoidal rule.

The hydration free enthalpy of hexanol and its solvation free enthalpy in octanol were calculated using a similar protocol for validation purposes, i.e., in order to have a set of independent free enthalpies to be compared with the results from the twin-system EDS approach. Due to a sharper variation of the Hamiltonian derivative between λ-values of 0.2 and 0.3 and between λ-values of 0.9 and 1.0 in the case of the octanol solvent, the number of λ-points was increased to 28 and the sampling period at each λ-point was increased to 3.6 ns after 0.4 ns equilibration. Graphs showing the average of the Hamiltonian derivative as function of λ are provided in Figure S2 of the Supporting Information.

EDS reference-state simulations were performed to calculate each of the six $\Delta\Delta G^{M\rightarrow X}_{O\rightarrow W}$ values according to eq 5. These simulations, involving fixed smoothness parameters and energy offsets, were carried out for a period of 10 ns (butane, pentane, and heptane), 15 ns (octane), and 30 ns (hexanol and 1,2-dimethoxyethane), respectively, after 1 ns equilibration. Energies were written to file every 2 ps. The EDS parameters were determined independently for each of the six calculations prior to the production simulations using the parameter update procedure described earlier.[16] The optimized values are listed in Table S2 of the Supporting Information.

The EDS reference-state simulations were conducted within a single-topology approach,[114] i.e., the change from the reference compound M to the target compound X is performed by changing the types of some of the atoms constituting a common core structure. For alchemical perturbations of hexane to other alkanes or to hexanol, the common core shared by the two end states corresponds to an aliphatic chain with the covalent interaction parameters specified in Figure S1 of the Supporting Information. The alchemical transformation of hexane to 1,2-dimethoxyethane involves contributions from a change of covalent interaction parameters.[115] Because the current implementation of EDS does not allow for a perturbation of these parameters, a modified aliphatic chain was used for the alchemical perturbation of hexane to 1,2-dimethoxyethane, with covalent interaction parameters appropriate for the 1,2-dimethoxyethane molecule. The hydration free enthalpy of this modified chain and its solvation free enthalpy in octanol were calculated with the same computational protocol as used for hexane (see above). It turns out, however, that the contributions from changing covalent interaction parameters essentially cancel out in the calculation of $\Delta\Delta G^{M\rightarrow X}_{O\rightarrow W}$. Graphs showing the average of the Hamiltonian derivative as function of λ are provided in Figure S3 of the Supporting Information.

3.3. Trajectory Analysis. The EDS reference-state trajectories were analyzed in terms of the time series of the potential energy difference between state B and state A, $\Delta V_{BA}(t) = V_B(t) - V_A(t)$, the distribution of this potential energy difference in the reference-state ensemble $\rho_R(\Delta V_{BA})$, the predicted potential energy difference distributions in the end-state ensembles, $\tilde{\rho}_A(\Delta V_{BA})$ and $\tilde{\rho}_B(\Delta V_{BA})$, and the predicted end-state solute−solute plus solute−solvent potential energy distribution $\tilde{\rho}_A(V_A)$ and $\tilde{\rho}_B(V_B)$.

Distributions $\rho_A(V_A)$ and $\rho_B(V_B)$ of solute−solute plus solute−solvent nonbonded energies were calculated for all end-state trajectories to compare them with corresponding reweighted end-state potential energy distributions $\tilde{\rho}_A(V_A)$ and $\tilde{\rho}_B(V_B)$ extracted from the EDS reference-state simulations. As the perturbations only involve the solute, solvent−solvent potential energy and entropic contributions exactly cancel out each other and can be omitted.[116−118] This analysis was carried out using the GROMOS++ suite of programs.[119]

4. RESULTS AND DISCUSSION

4.1. Free Enthalpies of Hydration and of Solvation in Octanol. In the context of partition coefficients, the free enthalpies appearing in eq 2 usually refer to mutually saturated octanol and water phases. While the properties of the water phase are not altered significantly by the very small equilibrium concentration of octanol,[20,120,121] the magnitude of the solvation free-enthalpy difference between dry and wet octanol

has been matter of controversy among different experimental studies.[120−123] It is consensual, however, that the free enthalpy of transfer from dry to wet octanol, $\Delta G_{dO\rightarrow wO}$, is favorable for polar alcohols and unfavorable for nonpolar molecules such as alkanes. The experimental data[23,123−126] selected in the present work for comparison with the calculated free enthalpies are presented in Table 1.

The calculated hydration free enthalpies of hexane and hexanol and their solvation free enthalpies in dry and wet octanol are also reported in Table 1. For hexane in water, good agreement is achieved between the calculated value of 10.5 ± 0.8 kJ mol^{-1} and the experimental[23] value of 10.4 kJ mol^{-1} as well as with the calculated value of 11.5 ± 0.5 kJ mol^{-1} reported by Schuler et al.[127] using the 45A3 force field, which has introduced the nonbonded interaction parameters for the aliphatic carbons still in use in the current force-field versions. For hexanol, the calculated values of −17.3 ± 0.9 (54A7) and −16.7 ± 0.8 kJ mol^{-1} (53A6$_{OXY}$) for the free enthalpy of hydration are also in good agreement with the experimental[23] value of −18.3 kJ mol^{-1} and with the earlier simulations of Horta et al.[81] using the 53A6 force field (identical to 54A7 for this compound) resulting in −16.6 ± 1.7 kJ mol^{-1}. The differences between 54A7 and 53A6$_{OXY}$ concerning the −CH$_2$−O−H headgroup of hexanol have only a weak effect on the free enthalpy of hydration.

The free enthalpy of solvation of −14.6 ± 1.0 kJ mol^{-1} (54A7) for hexane calculated in dry octanol is in agreement with the experimental value of −13.9 kJ mol^{-1} reported by Berti et al.[124] for dry octanol. For the transfer from dry to wet octanol, the simulation results suggest $\Delta G_{dO\rightarrow wO}$ = +1.4 kJ mol^{-1} (54A7) in reasonable agreement with the experimental estimate of +2.0 kJ mol^{-1} reported by Bernazzani et al.[123] Note, however, that another study[121] reports $\Delta G_{dO\rightarrow wO}$ values that are smaller than 1.0 kJ mol^{-1}. Other simulation studies show that the results of $\Delta G_{dO\rightarrow wO}$ calculations are sensitive to the force field used. The TIP4P/OPLS combination yields +0.1 to +0.2 kJ mol^{-1} along the series of solutes methane to butane,[62] while the SPC/TraPPE-UA combination leads to values of +0.8 to +1.6 kJ mol^{-1} for the series butane to octane.[78] The difference between the 54A7 and 53A6$_{OXY}$ force fields for the free enthalpy of solvation of hexane in wet octanol only concerns the representation of the solvent hydroxyl group and is found to be negligible. For hexanol, the calculated free enthalpy of solvation of −33.1 ± 1.6 kJ mol^{-1} (54A7) in dry octanol is significantly more negative than the estimated experimental value of −28.6 kJ mol^{-1} for dry octanol. For the transfer of hexanol from dry to wet octanol, the simulation results suggest $\Delta G_{dO\rightarrow wO}$ = +0.6 ± 2.3 kJ mol^{-1} (54A7). Other simulation studies report slightly negative values of about −1 kJ mol^{-1} along the series of solutes methanol to butanol.[62] Experimental estimates for the free enthalpy of transfer are somewhat ambiguous. Dallas and Carr report values from −0.7 to −0.4 kJ mol^{-1} for the series of solutes ethanol to pentanol,[121] while Cabani et al.[125] measured −1.76 kJ mol^{-1} and −1.36 kJ mol^{-1} for the solutes butanol and octanol, respectively. The difference between the 54A7 and 53A6$_{OXY}$ force fields for the solvation of hexanol in wet octanol concerns the representation of the solute and solvent hydroxyl groups and amounts to −1.5 kJ mol^{-1}. The value of −31.0 ± 1.6 kJ mol^{-1} for the free enthalpy of solvation of hexane in wet octanol calculated using the 53A6$_{OXY}$ force field is in very good agreement with the experimental value of −30.1 kJ mol^{-1} reported by Riebesehl and Tomlinson[126] for wet octanol. Expectedly, the agreement is less good for the 54A7 force field.

Also reported in Table 1 is the free enthalpy of hydration of hexane with modified torsional-energy parameters appropriate for the 1,2-dimethoxyethane molecule and its solvation free enthalpy in wet octanol. As expected, the results differ from those for normal hexane. However, when taking the difference between ΔG^{M}_{W} and ΔG^{M}_{O} (M = hexane$_{+D}$), the results for normal and modified hexane are essentially identical, showing that the normal hexane molecule could have been used as the reference solute for 1,2-dimethoxyethane as well.

4.2. Octanol−Water Partition Coefficients. The differences in the free enthalpy between the considered solutes and hexane for the transfer from water to octanol, $-\Delta\Delta G^{M\rightarrow X}_{O\rightarrow W}$, are reported in Table 2 for the 54A7 force field, evaluated in dry and wet octanol, and for the 53A6$_{OXY}$ force field, evaluated in wet octanol only. The reported numbers are calculated directly from the twin-system simulations using the EDS parameters listed in Table S2 of the Supporting Information. The difference between dry and wet octanol within the 54A7 force field are small and within the statistical uncertainties of the calculated numbers. The same holds for the comparison between the 54A7 and 53A6$_{OXY}$ versions applied to the wet octanol system.

Table 2. Differences in transfer free enthalpies between solute X and reference solute M[a]

	54A7		53A6$_{OXY(+D)}$
compound X	$-\Delta\Delta G^{M\rightarrow X}_{dO\rightarrow W}$	$-\Delta\Delta G^{M\rightarrow X}_{wO\rightarrow W}$	$-\Delta\Delta G^{M\rightarrow X}_{wO\rightarrow W}$
butane	7.6 ± 0.3	7.2 ± 0.3	7.2 ± 0.3
pentane	3.6 ± 0.2	3.8 ± 0.2	3.9 ± 0.2
heptane	−3.4 ± 0.2	−3.4 ± 0.2	−3.1 ± 0.2
octane	−7.6 ± 0.3	−6.9 ± 0.2	−6.9 ± 0.3
hexanol	9.3 ± 0.6	9.0 ± 0.3	9.2 ± 0.3
1,2-dimethoxy-ethane			26.7 ± 0.6[b]

[a]The values (in kJ mol^{-1}), based on a unit molarity (1 mol dm^{-3}) standard state for the two phases,[135] are directly obtained from EDS simulations in the twin-system setup, using the 54A7[79,80] or 53A6$_{OXY}$[81]/53A6$_{OXY+D}$[82] versions of the GROMOS force field. They account for the transfer process from water to octanol ($-\Delta\Delta G^{M\rightarrow X}_{O\rightarrow W} = \Delta G^{X}_{W\rightarrow O} - \Delta G^{M}_{W\rightarrow O}$). For the systems studied here, the reference solute M is hexane$_{(+D)}$, where the +D applies only to simulations involving 1,2-dimethoxyethane. [b]For this compound, an additional calculation considering an octanol−water mixture with a water mole fraction of 0.27 (experimental saturation concentration), instead of 0.16, resulted in $-\Delta\Delta G^{M\rightarrow X}_{wO\rightarrow W}$ = 26.0 ± 0.4 kJ mol^{-1}.

Figure 4 shows the energy-difference distributions obtained with the 53A6$_{OXY}$ force field in wet octanol for all perturbations except that involving 1,2-dimethoxyethane. For the latter system, the distributions are displayed in Figure 5. Corresponding graphs for the 54A7 force field in the dry and wet octanol systems are provided in Figures S4 and S5 of the Supporting Information.

In all cases, the energy-difference distributions exhibit a high-energy tail, essential for an accurate estimation of the free-enthalpy difference according to eq 5. Also shown in Figures 4 and 5 are the distributions of the solute−solute plus solute−solvent nonbonded energies obtained from the EDS reference-state trajectories via reweighting and from plain MD simulations of the various end states. In all cases, the EDS and plain MD end-state energy distributions are nearly

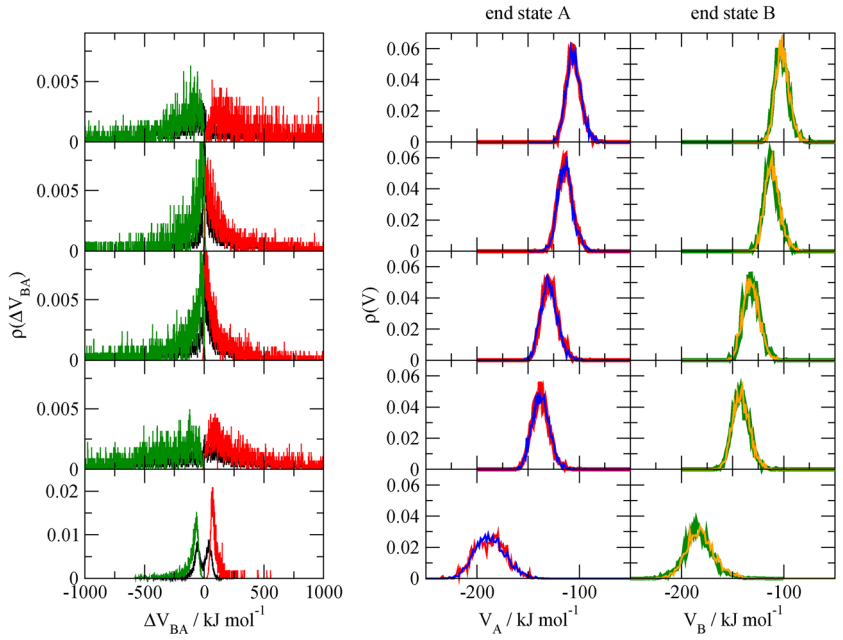

Figure 4. Left: Energy difference distributions for the reference state, $\rho_R(\Delta V_{BA})$ (black), and the two end states, $\tilde{\rho}_A(\Delta V_{BA})$ (red) and $\tilde{\rho}_B(\Delta V_{BA})$ (green), as obtained from twin-system EDS simulations. State B represents the combined Hamiltonians of solute X solvated in wet octanol (X = butane, pentane, heptane, octane, hexanol; from top to bottom) and solute M solvated in water (M = hexane). State A represents the combined Hamiltonians of solute X solvated in water and solute M solvated in wet octanol. The simulations were performed with the 53A6$_{OXY}$[81] force field. The energy difference distributions of the end states were determined by reweighting. Right: Nonbonded solute−solute plus solute−solvent energy distributions of the EDS end states obtained via reweighting from EDS reference-state simulations ($\tilde{\rho}_A(V_A)$ and $\tilde{\rho}_B(V_B)$, red and green) and from independent MD simulations of the end states ($\rho_A(V_A)$ and $\rho_B(V_B)$, blue and orange).

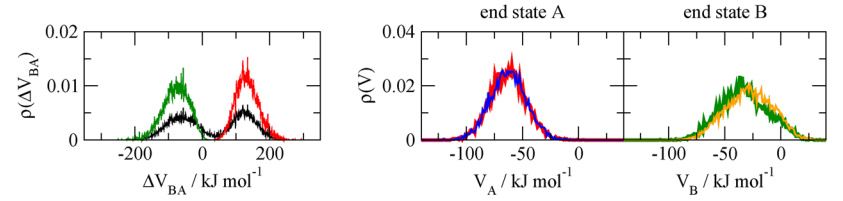

Figure 5. Left: Energy difference distributions for the reference state, $\rho_R(\Delta V_{BA})$ (black), and the two end states, $\tilde{\rho}_A(\Delta V_{BA})$ (red) and $\tilde{\rho}_B(\Delta V_{BA})$ (green), as obtained from twin-system EDS simulations. State B represents the combined Hamiltonians of solute 1,2-dimethoxyethane solvated in wet octanol and solute hexane solvated in water. State A represents the combined Hamiltonians of solute 1,2-dimethoxyethane solvated in water and solute hexane solvated in wet octanol. The simulations were performed with the 53A6$_{OXY+D}$[82] force field. The energy difference distributions of the end states were determined by reweighting. Right: Nonbonded solute−solute plus solute−solvent energy distributions of the EDS end states obtained via reweighting from EDS reference-state simulations ($\tilde{\rho}_A(V_A)$ and $\tilde{\rho}_B(V_B)$, red and green) and from independent MD simulations of the end states ($\rho_A(V_A)$ and $\rho_B(V_B)$, blue and orange).

identical, providing additional evidence that the parts of the phase space sampled in the end-state simulations were properly sampled in the EDS reference-state simulations. Figure 6 shows the time series of ΔV_{BA}, the difference of the end-state energies, in the six reference-state simulations. In all cases frequent transitions between the values corresponding to the two end states are observed. However, for the transformations of hexane to hexanol and hexane to 1,2-dimethoxyethane, the residence times in each state are significantly longer than for the transformations of hexane to the other alkanes.

The relative free enthalpies of transfer, $-\Delta\Delta G^{M\to X}_{O\to W}$, listed in Table 2 need to be subtracted from the difference of ΔG^M_W and ΔG^M_O obtained for the reference compound M (hexane), so as to obtain partition coefficients, which are reported in Table 3. A positive value of log P^X_{OW} reflects a higher affinity for the octanol phase compared to the water phase. The experimental data[20,128,129] reported in Table 3 refer to mutually saturated phases. The partition coefficients for hexane and hexanol from Table 3 (4.00 ± 0.25 and 2.03 ± 0.03, respectively) are compatible with the experimental free enthalpies of hydration of hexane and hexanol and their solvation free enthalpies in wet octanol selected for Table 1, which result in partition coefficients of 3.90 and 2.08 according to eq 2.

The results obtained with the 54A7 force field show that taking into account the residual hydration of octanol systematically improves the agreement with experimental data. Note that this improvement results mainly from the less negative free enthalpy of solvation of the reference compound hexane in wet octanol compared to dry octanol (Table 1), leading to a shift of all partition coefficients to lower values (decrease of log P_{OW} by about 0.2 to 0.3). This is illustrated graphically in Figure 7, showing that quantitative agreement with experimental data is only achieved for the simulation results obtained in wet octanol.

The performances of the 54A7 and 53A6$_{OXY}$ force fields are comparable for predicting the partition coefficients of the alkanes. For hexanol, both force fields overpredict the

dx.doi.org/10.1021/ct300933y | J. Chem. Theory Comput. 2013, 9, 1334−1346

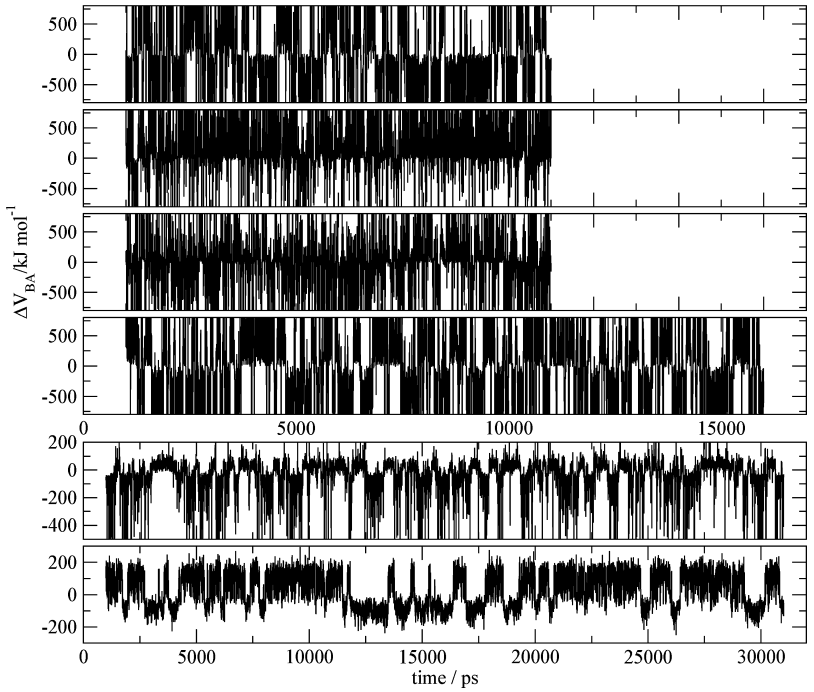

Figure 6. Time series of the energy difference $\Delta V_{BA} = V_B - V_A$ in twin-system EDS reference-state simulations coupling two simulation boxes containing one solute molecule solvated in water and wet octanol, respectively, using the 53A6$_{OXY}$[81] force field. State B represents the combined Hamiltonians of solute X solvated in wet octanol (X = butane, pentane, heptane, octane, hexanol, 1,2-dimethoxyethane; from top to bottom) and solute M solvated in water (M = hexane). State A represents the combined Hamiltonians of solute X solvated in water and solute M solvated in wet octanol. 1,2-dimethoxyethane was simulated using the 53A6$_{OXY+D}$[82] extension of the 53A6$_{OXY}$ force field.

Table 3. Octanol−Water Partition Coefficients of C_4 to C_8 *n*-Alkanes, Hexanol, and 1,2-Dimethoxyethane[a]

	log P^X_{OW}			
	54A7		53A6$_{OXY(+D)}$[b]	
compound X	dry octanol	wet octanol	wet octanol	exptl. (wet octanol)
butane	3.06 ± 0.22	2.89 ± 0.25	2.89 ± 0.23	2.89 ± 0.20[c]
pentane	3.76 ± 0.22	3.50 ± 0.24	3.46 ± 0.24	3.45 ± 0.20[d]
hexane[e,f]	4.39 ± 0.22	4.15 ± 0.24	4.15 ± 0.22	4.00 ± 0.25[d]
heptane	5.00 ± 0.22	4.75 ± 0.24	4.69 ± 0.22	4.50 ± 0.25[d]
octane	5.72 ± 0.22	5.36 ± 0.24	5.35 ± 0.23	5.15 ± 0.45[d]
hexanol	2.76 ± 0.25	2.58 ± 0.22	2.54 ± 0.23	2.03 ± 0.03[d]
hexanol[f]	2.76 ± 0.33	2.66 ± 0.33	2.50 ± 0.33	
1,2-dimethoxyethane			−0.40 ± 0.25[g]	−0.21 ± 0.02[h]

[a]The values are obtained from EDS simulations in the twin-system setup using the 54A7[79,80] force field for dry and wet octanol, the 53A6$_{OXY}$[81]/53A6$_{OXY+D}$[82] force field for wet octanol, and from experiment (exptl.). [b]The +D version applies only for 1,2-dimethoxyethane. [c]Ref 20, experimental uncertainty assumed to be equal to that for pentane. [d]Ref 129. [e]Reference compound. [f]Calculated directly from the TI results reported in Table 1. [g]For this compound, an additional calculation considering an octanol−water mixture with a water mole fraction of 0.27 (experimental saturation concentration), instead of 0.16, resulted in a partition coefficient of −0.26 ± 0.22. [h]Ref 128.

experimental partition coefficient of 2.03 ± 0.03 by 0.5 log *P* units. To exclude methodological reasons, the partition coefficient for hexanol was also calculated from the free enthalpies of hydration reported in Table 1. The results of 2.66 ± 0.33 for the 54A7 force field and 2.50 ± 0.33 for the 53A6$_{OXY}$ force field also overpredict the experimental partition coefficient. This suggests that the observed discrepancy relative to experimental values is due to force-field inaccuracies rather than to sampling problems. For 1,2-dimethoxyethane and wet octanol, the calculated value of −0.40 ± 0.25 is in good agreement with the experimental value of −0.21 ± 0.02 and also improved compared to the value of −0.68 previously calculated by Fuchs et al.[82] in dry octanol using the 53A6$_{OXY+D}$ force field. For a water mole fraction of 0.27 in the octanol phase, the calculated partition coefficient is −0.26 ± 0.22, very close to the experimental number.

For the alkanes, the present results show a slight overprediction of the increase in log P_{OW} with increasing number of carbon atoms, for the simulations in both dry and wet octanol. A similar trend was also reported for other force fields such as OPLS-AA and TraPPE, while simulated log P_{OW} values in dry octanol using a combination of different force fields, GROMOS 53A6 for water and OPLS-AA/TraPPE for the organic phase, were found to be in good agreement with experimental data[65] that were, however, determined for wet octanol. In the case of alkanes, reported estimates for partition coefficients in dry octanol differ from those measured in wet octanol only by about 0.2−0.3 log *P* units,[125] which is often within the error

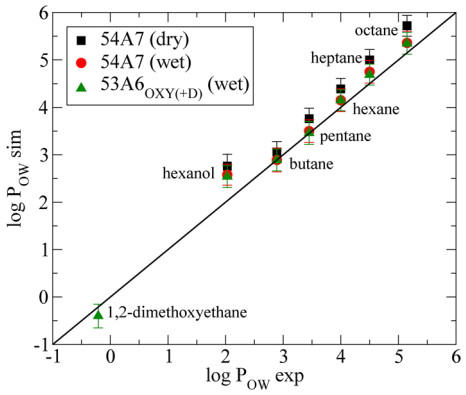

Figure 7. Comparison of simulated octanol–water partition coefficients using different force field versions or/and dry and wet octanol phases against experimental data.

affecting the calculated values. Nevertheless, the present results suggest that the appropriate comparison between simulation results and experimental data should be based on similar conditions in terms of the water content of the octanol phase.

4.3. Evaluation of the Twin-System Setup. In general, the computational effort of EDS compared to TI will depend on the degree of difference between the end-state Hamiltonians, on the choice of a λ-dependence for the Hamiltonian in TI, and on the required precision for the resulting free-enthalpy differences. For example, in the present case, the computational cost of calculating the partition coefficient for hexanol using TI amounted to 42 ns of simulation time for the box of water molecules and 112 ns for the box of octanol molecules, similar to simulation times used by others for similar systems.[65−67,70] The combination of TI and twin-system EDS proposed in this work required two times 42 ns for determining the hydration free enthalpy of hexane and its solvation free enthalpy in octanol and about 40 ns for the perturbation of hexane to hexanol using the twin-system EDS approach, including 10 ns for the EDS-parameter optimization. Considering that a twin-system simulation is about twice as expensive as a single-system one, the two approaches require similar computational effort for the calculation of the partition coefficient of a single arbitrary compound. However, for a series of closely related compounds for which a common model compound is adequate, the twin-system EDS approach becomes more efficient because no additional TI calculations are required. Future applications of this new methodology will show how large the differences between reference and target compounds can be for an efficient use of the twin-system setup.

A general advantage of EDS over other methods such as TI or FEP is the absence of any directionality of the process. For TI or FEP, the alchemical transformation can be carried out in a forward and a reverse direction that usually have different convergence properties leading to hysteresis.[130,131] Such an asymmetry is not present in EDS where the system can alternate smoothly between the two end states during the reference-state simulation. However, the extents of the relevant parts of phase space that need to be sampled will usually differ for the two end states. This is reflected in an asymmetric energy-difference distribution as illustrated in Figure 8a for the transformation of hexanol to hexane in water and in Figure 8b for the transformation of hexane to hexanol in wet octanol. In both cases, the sampling of the hexane end state allows the system to adopt a variety of high-energy configurations leading to high-energy tails in the distributions, while that of the hexanol end state shows a narrower range of possible energy differences.

The magnitude of the finite-sampling error[132] affecting the estimate of ΔG depends on whether the two ensemble averages in eq 5 have been sampled with the correct ratio. Frequent transitions between the two end states increase the likelihood that when sampling one end state, configurations important for the other one are encountered. However, in the case of asymmetric energy-difference distributions, the system with the more narrow distribution will be less likely to encounter configurations important to the other system, thus increasing the bias asymmetrically.[133,134] With the twin-system setup (Figure 1, bottom part), the two energy-difference distributions are more symmetric by construction compared to those of the individual perturbations, as illustrated in Figure 8c. As a result, the free-enthalpy estimates are expected to be less susceptible to statistical inaccuracies introduced by finite sampling.

5. CONCLUSION

The Enveloping Distribution Sampling (EDS) method has been extended to probe a single-simulation alternative to the thermodynamic cycle that is commonly used for measuring the effect of a modification of a chemical compound, e.g., from a given species to a chemical derivative for a ligand or solute molecule, on the free-enthalpy change associated with a change in environment, e.g., from the unbound state to the bound state

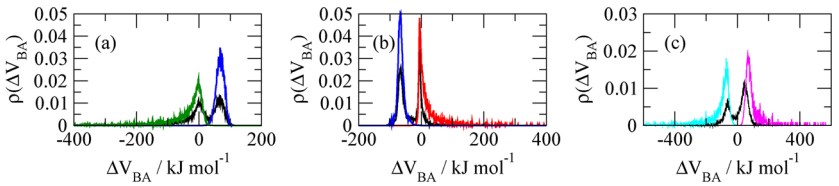

Figure 8. (a) Energy difference distributions for the reference state, $\rho_R(\Delta V_{BA})$ (black), and the two end states, $\tilde{\rho}_A(\Delta V_{BA})$ (blue) and $\tilde{\rho}_B(\Delta V_{BA})$ (green), associated with the alchemical transformation of hexanol (state A) to hexane (state B) in water as obtained from a single-system EDS simulation, using a smoothness parameter $s = 0.256$ and a relative energy offset $E^R_{BA} = +30.1$ kJ mol^{-1}. (b) Energy difference distributions for the reference state, $\rho_R(\Delta V_{BA})$ (black), and the two end states, $\tilde{\rho}_A(\Delta V_{BA})$ (red) and $\tilde{\rho}_B(\Delta V_{BA})$ (blue), associated with the alchemical transformation of hexane (state A) to hexanol (state B) in wet octanol as obtained from a single-system EDS simulation, using a smoothness parameter $s = 0.188$ and a relative energy offset $E^R_{BA} = +18.2$ kJ mol^{-1}. (c) Energy difference distributions for the reference state, $\rho_R(\Delta V_{BA})$ (black), and the two end states, $\tilde{\rho}_A(\Delta V_{BA})$ (cyan) and $\tilde{\rho}_B(\Delta V_{BA})$ (magenta), as obtained from a twin-system EDS simulation, using a smoothness parameter $s = 0.085$ and a relative energy offset $E^R_{BA} = +11.0$ kJ mol^{-1}. State A represents the combined Hamiltonians of hexanol solvated in water and hexane solvated in wet octanol. State B represents the combined Hamiltonians of hexanol solvated in wet octanol and hexane solvated in water. All simulations were performed with the 54A7[79,80] force field. All energy difference distributions of the end states were determined by reweighting.

for a protein−ligand system or from one solvent to another one for a solute molecule. This alternative approach relies on the coupled simulation of two systems (computational boxes) 1 and 2, and the method is therefore referred to as twin-system EDS. Systems 1 and 2 account for the two choices of environment. The end states of the alchemical perturbation for the twin system associate the two alternative forms X and Y of the molecule to systems 1 and 2 or 2 and 1, respectively. In this way, the processes of transforming one molecule into the other are carried out simultaneously in opposite directions in the two environments, leading to a change in free enthalpy that is smaller than for the two individual processes and to an energy-difference distribution that is more symmetric.

The method was introduced and applied to the calculation of octanol−water partition coefficients for short alkanes, hexanol, and 1,2-dimethoxyethane. It is observed in particular that for a comparison between experimental and calculated partition coefficients, the water content of the octanol phase has to be taken into account in the simulations.

Concerning the methodology, it is shown that the proposed twin-system strategy offers advantages over thermodynamic integration in terms of computational efficiency for applications such as screening of a set of compounds that can be related to one or a few common model compounds, thereby allowing for larger differences in the end states than could be sampled by free-energy perturbation.

For more biologically relevant applications such as host−guest binding, the advantage of this method is to be less susceptible to statistical inaccuracies compared to free-enthalpy estimates that are obtained as differences of two large numbers of comparable magnitudes calculated from separate simulations along the branches of the standardly used thermodynamic cycle. Future work concerning the twin-system EDS approach will focus on these types of systems.

■ ASSOCIATED CONTENT

Supporting Information

Relevant nonbonded interaction parameters, covalent interaction types, EDS reference-state parameters, average of the derivatives of the Hamiltonian, energy difference distributions, and nonbonded solute−solute plus solute−solvent energy distributions of the EDS end states. This material is available free of charge via the Internet at http://pubs.acs.org.

■ AUTHOR INFORMATION

Corresponding Author

*E-mail: wfvgn@igc.phys.chem.ethz.ch.

Notes

The authors declare no competing financial interest.

■ ACKNOWLEDGMENTS

The authors thank Clara Christ for setting the stage for EDS calculations and for her comments to the manuscript as well as Nathan Schmid for helping with the implementation of the twin-system setup. This work was financially supported by the National Center of Competence in Research (NCCR) in Structural Biology, by grant number 200020-137827 of the Swiss National Science Foundation, and by grant number 228076 of the European Research Council, which is gratefully acknowledged.

■ REFERENCES

(1) IUPAP:. *Physica (Amsterdam)* **1978**, *93A*, 1−60.
(2) IUPAC: *Quantities, Units and Symbols in Physical Chemistry*; Blackwell Scientific Publications: Oxford, U. K., 1988.
(3) Ytreberg, F. M.; Swendsen, R. H.; Zuckerman, D. M. *J. Chem. Phys.* **2006**, *125*, 184114.
(4) Chipot, C.; Pohorille, A. *Free Energy Calculations: Theory and Applications in Chemistry and Biology*; Springer: Berlin, 2007.
(5) Pohorille, A.; Jarzynski, C.; Chipot, C. *J. Phys. Chem. B* **2010**, *114*, 10235−10253.
(6) Christ, C. D.; Mark, A. E.; van Gunsteren, W. F. *J. Comput. Chem.* **2010**, *31*, 1569−1582.
(7) Liu, P.; Dehez, F.; Cai, W.; Chipot, C. *J. Chem. Theory Comput.* **2012**, *8*, 2606−2616.
(8) Kirkwood, J. G. *J. Chem. Phys.* **1935**, *3*, 300−313.
(9) Zwanzig, R. W. *J. Chem. Phys.* **1954**, *22*, 1420−1426.
(10) Christ, C. D.; van Gunsteren, W. F. *J. Chem. Phys.* **2007**, *126*, 184110.
(11) Christ, C. D.; van Gunsteren, W. F. *J. Chem. Phys.* **2008**, *128*, 174112.
(12) Christ, C. D.; van Gunsteren, W. F. *J. Chem. Theory Comput.* **2009**, *5*, 276−286.
(13) Christ, C. D.; van Gunsteren, W. F. *J. Comput. Chem.* **2009**, *30*, 1664−1679.
(14) Riniker, S.; Christ, C. D.; Hansen, N.; Mark, A. E.; Nair, P. C.; van Gunsteren, W. F. *J. Chem. Phys.* **2011**, *135*, 024105.
(15) Lin, Z.; Liu, H.; Riniker, S.; van Gunsteren, W. F. *J. Chem. Theory Comput.* **2011**, *7*, 3884−3897.
(16) Hansen, N.; Dolenc, J.; Knecht, M.; Riniker, S.; van Gunsteren, W. F. *J. Comput. Chem.* **2012**, *33*, 640−651.
(17) Leeson, P. D.; Springthorpe, B. *Nat. Rev. Drug Discovery* **2007**, *6*, 881−890.
(18) Edwards, M. P.; Price, D. A. *Annu. Rep. Med. Chem.* **2010**, *45*, 381−391.
(19) Cronin, D.; Mark, T. *Curr. Comput.-Aided Drug Des.* **2006**, *2*, 405−413.
(20) Sangster, J. *Octanol-Water Partitioning Coefficients: Fundamentals and Physical Chemistry*; John Wiley and Sons: Chichester, U. K., 1997.
(21) Fredenslund, A.; Gmehling, J.; Rasmussen, P. *Vapor-Liquid Equilibria Using UNIFAC - a Group-Contribution Method*; Elsevier: Amsterdam, 1977.
(22) Rekker, R. F.; Kort, H. M. D. *Eur. J. Med. Chem.* **1979**, *14*, 479−488.
(23) Cabani, S.; Gianni, P.; Mollica, V.; Lepori, L. *J. Solution Chem.* **1981**, *10*, 563−595.
(24) Hirose, C.; Sepuldeva, L. *J. Phys. Chem.* **1981**, *85*, 3689−3694.
(25) Banerjee, S.; Howard, P. H. *Environ. Sci. Technol.* **1988**, *22*, 839−841.
(26) Klopman, G.; Li, J.-Y.; Wang, S.; Dimayuga, M. *J. Chem. Inf. Comput. Sci.* **1994**, *34*, 752−781.
(27) Smith, G. A.; Christian, S. D.; Tucker, E. E. *Langmuir* **1997**, *3*, 598−599.
(28) Wienke, G.; Gmehling, J. *Toxicol. Environ. Chem.* **1998**, *65*, 57−86.
(29) Klopman, G.; Namboodiri, K.; Schochet, M. *J. Comput. Chem.* **1985**, *6*, 28−38.
(30) Bodor, N.; Gabanyi, Z.; Wong, C. K. *J. Am. Chem. Soc.* **1989**, *111*, 3783−3786.
(31) Abraham, M. H.; Chadha, H. S.; Whiting, G. S.; Mitchell, R. C. *J. Pharm. Sci.* **1994**, *83*, 1085−1100.
(32) Hansch, C.; Leo, A. *Exploring QSAR: Fundamentals and Applications in Chemistry and Biology*; American Chemical Society: Washington, DC, 1995.
(33) Quina, F. H.; Alonso, E. O.; Farah, J. P. S. *J. Phys. Chem.* **1995**, *99*, 11708−11714.
(34) Hawkins, G. D.; Liotard, D. A.; Cramer, C. J.; Truhlar, D. G. *J. Org. Chem.* **1998**, *63*, 4305−4313.
(35) Rodrigues, M. A.; Alonso, E. O.; Yihwa, C.; Farah, J. P. S.; Quina, F. H. *Langmuir* **1999**, *15*, 6770−6774.

(36) Treiner, C.; Chattopadhyay, A. K. *J. Colloid Interface Sci.* **1986**, *109*, 101−108.
(37) Best, S. A.; Merz, K. M.; Reynolds, C. H. *J. Phys. Chem. B* **1999**, *103*, 714−726.
(38) Klamt, A.; Eckert, F. *Fluid Phase Equilib.* **2000**, *172*, 43−72.
(39) Buggert, M.; Mokrushina, L.; Smirnova, I.; Schomäcker, R.; Arlt, W. *Chem. Eng. Technol.* **2006**, *29*, 567−573.
(40) Nicholls, A.; Mobley, D. L.; Guthrie, J. P.; Chodera, J. D.; Bayly, C. I.; Cooper, M. D.; Pande, V. S. *J. Med. Chem.* **2008**, *51*, 769−779.
(41) Chen, Z.; Baker, N. A.; Wei, G. W. *J. Comput. Phys.* **2010**, *229*, 8231−8258.
(42) Chen, Z.; Baker, N. A.; Wei, G. W. *J. Math. Biol.* **2011**, *63*, 1139−1200.
(43) Palmer, D. S.; Frolov, A. I.; Ratkova, E. L.; Fedorov, M. V. *Mol. Pharmaceutics* **2011**, *8*, 1423−1429.
(44) Hempel, S.; Fischer, J.; Paschek, D.; Sadowski, G. *Soft Mater.* **2012**, *10*, 26−41.
(45) Case, F. H.; Chaka, A.; Moore, J. D.; Mountain, R. D.; Olson, J. D.; Ross, R. B.; Schiller, M.; Shen, V. K.; Stahlberg, E. A. *Fluid Phase Equilib.* **2009**, *285*, 1−3.
(46) Maginn, E. J. *AIChE J.* **2009**, *55*, 1304−1310.
(47) Johnson, S. R. *J. Chem. Inf. Model.* **2008**, *48*, 25−26.
(48) König, G.; Boresch, S. *J. Phys. Chem. B* **2009**, *113*, 8967−8974.
(49) Gmehling, J. *Fluid Phase Equilib.* **1998**, *144*, 37−47.
(50) Buggert, M.; Cadena, C.; Mokrushina, L.; Smirnova, I.; Maginn, E. J.; Arlt, W. *Chem. Eng. Technol.* **2009**, *32*, 977−986.
(51) Wille, S.; Buggert, M.; Mokrushina, L.; Arlt, W.; Smirnova, I. *Chem. Eng. Technol.* **2010**, *33*, 1075−1082.
(52) Mehling, T.; Ingram, T.; Smirnova, I. *Langmuir* **2012**, *28*, 118−124.
(53) Jämbeck, J. P. M.; Mocci, F.; Lyubartsev, A. P.; Laaksonen, A. *J. Comput. Chem.* **2013**, *34*, 187−197.
(54) Costa Gomes, M. F.; Pádua, A. A. H. In *Development and Applications in Solubility*; Letcher, T. M., Ed.; Royal Society of Chemistry: Cambridge, U. K., 2007; pp 153−170.
(55) Dohnal, V. In *Measurement of the Thermodynamic Properties of Multiple Phases*; Weir, R. D., de Loos, T. W., Eds.; Elsevier: Amsterdam, 2005; pp 359−381.
(56) Panagiotopoulos, A. Z. *Mol. Phys.* **1987**, *61*, 813−826.
(57) Panagiotopoulos, A. Z.; Quirke, N.; Stapleton, M. R.; Tildesley, D. J. *Mol. Phys.* **1988**, *63*, 527−545.
(58) Siepmann, J. I.; Frenkel, D. *Mol. Phys.* **1992**, *75*, 59−70.
(59) Frenkel, D.; Mooij, G. C. A. M.; Smit, B. *J. Phys.: Condens. Matter* **1992**, *4*, 3053−3076.
(60) Martin, M. G.; Siepmann, J. I. *J. Phys. Chem. B* **1999**, *103*, 4508−4517.
(61) Chen, B.; Siepmann, J. I. *J. Am. Chem. Soc.* **2000**, *122*, 6464−6467.
(62) Chen, B.; Siepmann, J. I. *J. Phys. Chem. B* **2006**, *110*, 3555−3563.
(63) Martin, M. G.; Siepmann, J. I. *Theor. Chem. Acc.* **1998**, *99*, 347−350.
(64) Martin, M. G.; Siepmann, J. I. *J. Phys. Chem. B* **1999**, *103*, 11191−11195.
(65) Garrido, N. M.; Queimada, A. J.; Jorge, M.; Macedo, E. A.; Economou, I. G. *J. Chem. Theory Comput.* **2009**, *5*, 2436−2446.
(66) Garrido, N. M.; Jorge, M.; Queimada, A. J.; Macedo, E. A.; Economou, I. G. *Chem. Phys. Phys. Chem.* **2011**, *13*, 9155−9164.
(67) Garrido, N. M.; Economou, I. G.; Queimada, A. J.; Jorge, M.; Macedo, E. A. *AIChE J.* **2012**, *58*, 1929−1938.
(68) van Gunsteren, W. F. In *Computer Simulation of Biomolecular Systems, Theoretical and Experimental Applications*; van Gunsteren, W. F., Weiner, P. K., Eds.; Escom Science Publishers: Leiden, The Netherlands, 1989; pp 27−59.
(69) Mark, A. E.; van Helden, S. P.; Smith, P. E.; Janssen, L. H. M.; van Gunsteren, W. F. *J. Am. Chem. Soc.* **1994**, *116*, 6293−6302.
(70) Economou, I. G.; Garrido, N. M.; Makrodimitri, Z. A. *Fluid Phase Equilib.* **2010**, *296*, 125−132.
(71) Essex, J. W.; Reynolds, C. A.; Richards, W. G. *J. Chem. Soc., Chem. Commun.* **1989**, 1152−1154.
(72) Jorgensen, W. L.; Briggs, J. M.; Contreras, M. L. *J. Phys. Chem.* **1990**, *94*, 1683−1686.
(73) Mordasini, T. Z.; McCammon, J. A. *J. Phys. Chem. B* **2000**, *104*, 360−367.
(74) Jorgensen, W. L.; Thomas, L. L. *J. Chem. Theory Comput.* **2008**, *4*, 869−876.
(75) Lyubartsev, A. P.; Jacobsson, S. P.; Sundholm, G.; Laaksonen, A. *J. Phys. Chem. B* **2001**, *105*, 7775−7782.
(76) Khavrutskii, I. V.; Wallqvist, A. *J. Chem. Theory Comput.* **2010**, *6*, 3427−3441.
(77) Kamath, G.; Bhatnagar, N.; Baker, G. A.; Baker, S. N.; Potoff, J. J. *Phys. Chem. Chem. Phys.* **2012**, *14*, 4339−4342.
(78) Bhatnagar, N.; Kamath, G.; Chelst, I.; Potoff, J. J. *J. Chem. Phys.* **2012**, *137*, 014502.
(79) Poger, D.; van Gunsteren, W. F.; Mark, A. E. *J. Comput. Chem.* **2010**, *31*, 1117−1125.
(80) Schmid, N.; Eichenberger, A.; Choutko, A.; Riniker, S.; Winger, M.; Mark, A. E.; van Gunsteren, W. F. *Eur. Biophys. J.* **2011**, *40*, 843−856.
(81) Horta, B. A. C.; Fuchs, P. F. J.; van Gunsteren, W. F.; Hünenberger, P. H. *J. Chem. Theory Comput.* **2011**, *7*, 1016−1031.
(82) Fuchs, P. F. J.; Hansen, H. S.; Hünenberger, P. H.; Horta, B. A. C. *J. Chem. Theory Comput.* **2012**, *8*, 3943−3963.
(83) Torrie, G. M.; Valleau, J. P. *J. Comput. Phys.* **1977**, *23*, 187−199.
(84) Han, K. K. *Phys. Lett. A* **1992**, *165*, 28−32.
(85) Han, K. K. *Phys. Rev. E* **1996**, *54*, 6906−6910.
(86) Chen, Y. G.; Hummer, G. *J. Am. Chem. Soc.* **2007**, *129*, 2414−2415.
(87) Jacucci, G.; Quirke, N. *Lect. Notes Phys.* **1982**, *166*, 38−57.
(88) Powles, J. G.; Evans, W. A. B.; Quirke, N. *Mol. Phys.* **1982**, *46*, 1347−1370.
(89) Salsburg, Z. W.; Jacobson, J. D.; Fickett, W.; Wood, W. W. *J. Chem. Phys.* **1959**, *30*, 65−72.
(90) Ferrenberg, A. M.; Swendsen, R. H. *Phys. Rev. Lett.* **1988**, *61*, 2635−2638.
(91) Wu, D.; Kofke, D. A. *J. Chem. Phys.* **2005**, *123*, 054103.
(92) Schmid, N.; Christ, C. D.; Christen, M.; Eichenberger, A. P.; van Gunsteren, W. F. *Comput. Phys. Commun.* **2012**, *183*, 890−903.
(93) Kunz, A. P. E.; Allison, J. R.; Geerke, D. P.; Horta, B. A. C.; Hünenberger, P. H.; Riniker, S.; Schmid, N.; van Gunsteren, W. F. *J. Comput. Chem.* **2012**, *33*, 340−353.
(94) Riniker, S.; Christ, C. D.; Hansen, H. S.; Hünenberger, P. H.; Oostenbrink, C.; Steiner, D.; van Gunsteren, W. F. *J. Phys. Chem. B* **2011**, *115*, 13570−13577.
(95) Biomolecular Simulation - The GROMOS Software. http://www.gromos.net (accessed Jan. 2013).
(96) Oostenbrink, C.; Villa, A.; Mark, A. E.; van Gunsteren, W. F. *J. Comput. Chem.* **2004**, *25*, 1656−1676.
(97) Berendsen, H. J. C.; Postma, J. P. M.; van Gunsteren, W. F.; Hermans, J. In *Intermolecular Forces*; Pullmann, B., Ed.; Reidel: Dordrecht, The Netherlands, 1981; pp 331−342.
(98) MacCallum, J. L.; Tieleman, D. P. *J. Am. Chem. Soc.* **2002**, *124*, 15085−15093.
(99) Hockney, R. W. *Methods Comput. Phys* **1970**, *9*, 136−211.
(100) Ryckaert, J.-P.; Ciccotti, G.; Berendsen, H. J. C. *J. Comput. Phys.* **1977**, *23*, 327−341.
(101) Berendsen, H. J. C.; Postma, J. P. M.; van Gunsteren, W. F.; DiNola, A.; Haak, J. R. *J. Chem. Phys.* **1984**, *81*, 3684−3690.
(102) Kell, G. S. *J. Chem. Eng. Data* **1967**, *12*, 66−69.
(103) Riddick, J. A.; Bunger, W. B.; Sakand, T. K. *Organic Solvents: Physical Properties and Methods of Purification*; Wiley: New York, 1986.
(104) Berendsen, H. J. C. In *Molecular Dynamics and Protein Structure*; Hermans, J., Ed.; Polycrystal Book Service: Western Springs, IL, 1985; pp 18−22.
(105) Barker, J. A.; Watts, R. O. *Mol. Phys.* **1973**, *26*, 789−792.
(106) Tironi, I. G.; Sperb, R.; Smith, P. E.; van Gunsteren, W. F. *J. Chem. Phys.* **1995**, *102*, 5451−5459.

(107) Wohlfarth, C. In *Landolt-Börnstein. Numerical Data and Functional Relationships in Science and Technology. Group IV: Macroscopic and Technical Properties of Matter*; Madelung, O., Ed.; Springer: Berlin, 1991; Vol. *6*; p 163.
(108) Lippold, B. C.; Adel, M. S. *Arch. Pharm. Pharm. Med. Chem.* **1972**, *305*, 417−426.
(109) D'Aprano, A.; Donato, D. I.; Caponetti, E. *J. Solution Chem.* **1979**, *8*, 135−146.
(110) Gestblom, B.; Sjöblom, J. *Acta Chem. Scand.* **1984**, *A38*, 47−56.
(111) Christen, M.; Hünenberger, P. H.; Bakowies, D.; Baron, R.; Bürgi, R.; Geerke, D. P.; Heinz, T. N.; Kastenholz, M. A.; Kräutler, V.; Oostenbrink, C.; Peter, C.; Trzesniak, D.; van Gunsteren, W. F. *J. Comput. Chem.* **2005**, *26*, 1719−1751.
(112) Beutler, T. C.; Mark, A. E.; van Schaik, R. C.; Gerber, P. R.; van Gunsteren, W. F. *Chem. Phys. Lett.* **1994**, *222*, 529−539.
(113) Allen, M. P.; Tildesley, D. J. *Computer Simulation of Liquids*; Oxford University Press: New York, 1987.
(114) Pearlman, D. A. *J. Phys. Chem.* **1994**, *98*, 1487−1493.
(115) Pearlman, D. A.; Kollman, P. A. *J. Chem. Phys.* **1991**, *94*, 4532−4545.
(116) Yu, H.-A.; Karplus, M. *J. Chem. Phys.* **1988**, *89*, 2366−2379.
(117) Peter, C.; Oostenbrink, C.; van Dorp, A.; van Gunsteren, W. F. *J. Chem. Phys.* **2004**, *120*, 2652−2661.
(118) van Gunsteren, W. F.; Geerke, D. P.; Trzesniak, D.; Oostenbrink, C.; van der Vegt, N. F. A. In *Protein Folding and Drug Design, Proceedings of the International School of Physics "Enrico Fermi", course CLXV*; Broglia, R. A., Serrano, L., Tiana, G., Eds.; IOS Press: Amsterdam - SIF, Bologna, 2007; pp 177−191.
(119) Eichenberger, A. P.; Allison, J. R.; Dolenc, J.; Geerke, D. P.; Horta, B. A. C.; Meier, K.; Oostenbrink, C.; Schmid, N.; Steiner, D.; Wang, D.; van Gunsteren, W. F. *J. Chem. Theory Comput.* **2011**, *7*, 3379−3390.
(120) Schantz, M. M.; Martire, D. E. *J. Chromatogr.* **1987**, *391*, 35−51.
(121) Dallas, A. J.; Carr, P. W. *J. Chem. Soc., Perkin Trans. 2* **1992**, 2155−2161.
(122) Berti, P.; Cabani, S.; Conti, G.; Mollica, V. *Thermochim. Acta* **1987**, *122*, 1−8.
(123) Bernazzani, L.; Cabani, S.; Conti, G.; Mollica, V. *J. Chem. Soc. Faraday Trans.* **1995**, *91*, 649−655.
(124) Berti, P.; Cabani, S.; Conti, G.; Mollica, V. *J. Chem. Soc. Faraday Trans. 1* **1986**, *82*, 2547−2556.
(125) Cabani, S.; Conti, G.; Mollica, V.; Bernazzani, L. *J. Chem. Soc. Faraday Trans.* **1991**, *87*, 2433−2442.
(126) Riebesehl, W.; Tomlinson, E. *J. Solution Chem.* **1986**, *15*, 141−150.
(127) Schuler, L. D.; Daura, X.; van Gunsteren, W. F. *J. Comput. Chem.* **2001**, *22*, 1205−1218.
(128) Funasaki, N.; Hada, S.; Neya, S.; Machida, K. *J. Phys. Chem.* **1984**, *88*, 5786−5790.
(129) Sangster, J. *J. Phys. Chem. Ref. Data* **1989**, *18*, 1111−1229.
(130) Lu, N.; Kofke, D. A. *J. Chem. Phys.* **2001**, *114*, 7303−7311.
(131) Wu, D.; Kofke, D. A. *J. Chem. Phys.* **2004**, *121*, 8742−8747.
(132) Wood, R. H.; Mühlbauer, W. C. F.; Thompson, P. T. *J. Phys. Chem.* **1991**, *95*, 6670−6675.
(133) Wu, D.; Kofke, D. A. *Phys. Rev. E* **2004**, *70*, 066702.
(134) Kofke, D. A. *Mol. Phys.* **2006**, *104*, 3701−3708.
(135) Ben-Naim, A. *J. Phys. Chem.* **1978**, *82*, 792−803.